Blockade of Vascular Endothelial Growth Factor Activity Suppresses Wear Debris-Induced Inflammatory Osteolysis

WEIPING REN, RENWEN ZHANG, DAVID C. MARKEL, BIN WU, XIN PENG, MONICA HAWKINS, and PAUL H. WOOLEY

ABSTRACT. ***Objective.*** Aseptic loosening is a common complication of total joint replacement in humans. Our study examined the hypothesis that wear debris may influence vascular endothelial grow factor (VEGF) expression, and that blocking VEGF bioactivity might improve wear debris-induced inflammatory osteolysis in a mouse model.

Methods. Ultra high molecular weight polyethylene (UHMWPE) particles were introduced into established air pouches on BALB/c mice, followed by implantation of calvaria bone from syngeneic littermates. Mice were treated with recombinant VEGF, or VEGF inhibitor (VEGF R2/F_c chimera) or vehicle control, and mice without UHMWPE stimulation were also included. Pouch tissues were harvested 2 weeks after bone implantation for molecular and histological analyses.

Results. Exposure of UHMWPE particles increased VEGF expression at both mRNA and protein levels in pouch tissues. Immunostaining revealed intense VEGF staining predominantly in UHMWPE deposit foci surrounded by inflammatory cells. VEGF inhibitor treatment strongly attenuated tissue inflammation (cellular infiltration, membrane proliferation, and expression of interleukin 1ß and tumor necrosis factor-α in UHMWPE-stimulated pouch tissues). Further, VEGF inhibitor treatment caused a significant reduction in the number of TRAP+ cells, and effectively prevented UHMWPE particle-induced bone resorption of implanted calvaria (assessed by extent of collagen depletion and frequency of bone erosions).

Conclusion. The observation that VEGF inhibitor treatment prevented UHMWPE particle-induced inflammatory osteolysis opens new possibilities for treatment of aseptic loosening, especially at an early stage. (J Rheumatol 2007;34:27–35)

Key Indexing Terms:
HIP REPLACEMENT ARTHROPLASTY
VASCULAR ENDOTHELIAL GROWTH FACTOR
OSTEOLYSIS
ANIMAL DISEASE MODELS

The number of total joint replacements performed in the USA is estimated at one-half million annually. Aseptic loosening (AL) due to osteolysis induced by wear debris is the most common cause of implant failure[1,2]. Cellular mechanisms related to AL pathology are relevant both for identifying patients at risk and developing novel treatment strategies. AL is characterized by the formation of a chronic inflammatory response to wear debris shed from the bone-implant interface, leading to bone resorption (osteolysis) and loss of fixation[3]. The periprosthetic tissue at the bone-implant interface shows a high degree of vascularization[4]. A number of factors contribute to angiogenesis; one of these, vascular endothelial growth factor (VEGF), is produced by multiple cell types such as macrophage and osteoblasts[5,6]; it represents an important mitogen for endothelial cells. VEGF gene expression is regulated by growth factors, hormones, and cytokines[6-9]. VEGF exerts its biological activity through binding to 2 receptors, VEGF receptor-1 (VEGFR-1; Flt-1) and VEGFR-2 (Flk-1/KDR)[10]. VEGF is actively involved in the process of inflammation[11], osteoclastogenesis[12,13], and bone resorption[13]. However, the role of VEGF in wear debris-induced inflammatory osteolysis has not been examined.

We recently developed a mouse osteolysis model[14] that allows us to quantitatively evaluate the molecular and histology profiles of wear debris-induced inflammation, osteoclastogenesis, and osteolysis under controlled experimental conditions. Our study examined the hypothesis that wear debris may influence VEGF expression, and that blocking of VEGF bioactivity may improve wear debris-induced inflammatory osteolysis in this model.

From the Department of Orthopaedic Surgery, Wayne State University (WSU) School of Medicine, Detroit, Michigan, and Stryker Company, Rutherford, New Jersey, USA.

Supported by the Stryker Company.

W. Ren, MD, PhD, Department of Orthopaedic Surgery, WSU School of Medicine; R. Zhang, MD, Stryker Company; D.C. Markel, MD; B. Wu, MD; X. Peng, MD, Department of Orthopaedic Surgery, WSU School of Medicine; M. Hawkins, PhD, Stryker Company; P.H. Wooley, PhD, Department of Orthopaedic Surgery, WSU School of Medicine.

Address reprint requests to Dr. W. Ren, Department of Orthopaedic Surgery, Wayne State University School of Medicine, University Health Center 7C, 4201 St. Antoine Blvd., Detroit, MI 48201.
E-mail: wren@med.wayne.edu

Accepted for publication July 17, 2006.

MATERIALS AND METHODS

Ultra high molecular weight polyethylene particles. High molecular weight polyethylene (UHMWPE) particles were the generous gift of Dr. John Cuckler (University of Alabama, Birmingham, AL, USA). Scanning electron microscopy analysis demonstrated that 90% of the UHMWPE particles were < 5.5 μm in diameter, with a mean size of 2.6 μm (range < 0.6 μm to 21 μm)[15]. UHMWPE particles were washed in 70% ethanol solution and resuspended in sterile phosphate buffered saline (PBS). The particle suspension was determined to be endotoxin-free by the Limulus assay (Endosafe; Charles Rivers, Charlestown, SC, USA).

Mouse osteolysis model. The murine model was used according to detailed protocol as described[14], and institutional approval was obtained for all animal procedures. A detailed description of study design and the method of drug administration are shown in Table 1. Air pouches were generated on female BALB/c mice (age 8–10 weeks; Jackson Laboratory, Bar Harbor, ME, USA). Six days later, mice with established air pouches were anesthetized by intraperitoneal injection of pentobarbital (50 mg/kg; Fisher Scientific, Pittsburgh, PA, USA). An incision of 0.5 cm overlying the pouch was made, and a section of calvaria bone from syngeneic littermates was surgically removed (about 0.4 × 0.25 cm) and inserted into the pouch using a sterile procedure. The pouch layers and the skin incision were then closed using 4-0 Prolene sutures. On the following day, pouches were injected with 0.5 ml saline containing UHMWPE particles (10 mg/ml). Pouches injected with saline alone were used as controls. Each experimental group comprised 10 mice. Mice were sacrificed in a carbon dioxide chamber 2 weeks after bone implantation. The pouch membranes containing implanted bone were harvested. A small portion of the pouch tissue was collected for molecular analysis. The remainder of the pouch tissue, with the intact bone implant, was either snap-frozen for crystallized sectioning, or fixed in 10% buffered formalin for paraffin embedding.

Drug treatment. Both recombinant human VEGF 165 (293-VE, a 42-kDa peptide with 97% homology to rabbit VEGF) and VEGF R2/F_c chimera (357-KD, a 110-kDa peptide containing the extracellular domain of a VEGF receptor linked to an IgG, which binds and inactivates free VEGF) were purchased from R&D Systems (Minneapolis, MN, USA). One hundred microliters of either VEGF or EGF R2/F_c chimera (1 μl/ml suspended in PBS with 0.1% bovine serum albumin, final concentration 5 μl/kg/day) were injected into the pouch tissue daily 2 days before UHMWPE injection.

Histological evaluation and image analysis. Pouch tissues were fixed in 10% formalin. After decalcification in 10% EDTA, specimens were processed for paraffin embedding and cutting by microtome. Tissue sections (6 μm) were stained with hematoxylin and eosin (H&E) to evaluate general histology, and 4 separate sections per specimen were evaluated in a blinded fashion. Digital images were acquired using a Zeiss light microscope equipped with a Toshiba CCD, and analyzed using the Image Pro software package (Media Cybernetics, Silver Spring, MD, USA). Pouch membrane thickness was determined at 6 points on each section, with an even distribution of measurements on the proximal side, distal side, and transition curve of the pouch. The total number of cells (based upon nucleus count) was analyzed as described[14,16]. Van Gieson stain was used to determine the implanted bone collagen content, and bone collagen depletion was determined by image analysis[14]. Briefly, images of modified Van Gieson-stained pouches with calvaria, at ×100 magnification, were analyzed with the software package (Image-Pro Plus). Integrated optical densities (IOD) of the areas at the bone surface contiguous with particles containing inflammatory pouch membranes were recorded and normalized, with the IOD measured at the same-sized inner part of the bone distal from the inflammatory membrane. Normalization of IOD of bone surface areas in contact with inflammatory membranes with IOD from the bone areas of the same section, but located away from the membranes, provided an accurate measurement that avoided possible differences due to section thickness and staining time variance. The obtained ratio was expressed as percentage of collagen content preserved in response to particle-stimulated inflammation. Six pairs of IOD readings at different regions of each bone section were determined in a minimum of 8 mice per group. Osteoclast-like cells in the pouch tissue were identified by tartrate-resistant acid phosphatase (TRAP, EC3.1.3.2) stain using a commercial kit (Sigma)[17]. Briefly, cryosections of pouch tissues (6 μm) were prepared and fixed in buffered acetone for 30 s. Sections were incubated at 37°C for 1 hour in 100 mM acetate buffer (pH 5.2), containing 0.5 mM naphthol AS-BI phosphoric acid, 2.2 mM Fast Garnet GBC, and 8 mM sodium tartrate. The sections were then washed in several changes of distilled water, followed by brief counterstaining with hematoxylin, and mounted in Crystal mount (Biomeda). The presence of dark purple staining granules in the cytoplasm was considered as the specific criterion for TRAP+ cells. Positive TRAP localization was quantified by pixel area count and reported as a percentage of the total implanted bone area in the pouch tissue.

Table 1. Study design and method of administration.

Group	n	Treatment
I	10	PBS (saline control)
II	10	PBS + VEGF (5 μg/kg/day, intra-pouch injection)
III	10	UHMWPE (0.5 mg per pouch)
IV	10	UHMWPE + VEGF (5 μg/kg/day, intra-pouch injection)
V	10	UHMWPE + VEGF inhibitor (VEGF F2/Fc chimera protein, 5 μg/kg/day, intra-pouch injection)

PBS: phosphate buffered saline; VEGF: vascular endothelial growth factor; UHMWPE: ultra high molecular weight polyethylene.

Immunohistological staining for VEGF, interleukin 1ß (IL-1ß), and tumor necrosis factor-α (TNF-α). Paraffin tissue sections were deparaffinized. Rinsed sections were immersed in antigen retrieval buffer (BioGenex, San Ramon, CA, USA), heated by microwave (600 kW for 2 min, followed by 300 kW for 5 min), and allowed to cool to room temperature. Sections were blocked with 1.5% normal goat serum for 1 h, and incubated overnight with rabbit anti-mouse VEGF and goat anti-mouse IL-1ß and TNF-α antibodies (2 μg/ml; Santa Cruz Biotechnology, Santa Cruz, CA, USA) at 4°C. After rinsing, sections were treated with biotinylated secondary antibody against either rabbit or goat IgG (Vector Laboratories). As for control, primary antibodies were replaced with nonimmune mouse IgG. After the reactions, the sections were incubated with avidin-biotin-peroxidase complex, and color was developed with 3.3'-diaminobezidine tetrahydrochloride (DAB). Digital images of representative fields of view were captured and analyzed using the Image-Pro software package. Computerized image analysis was used to analyze stained sections to obtain the percentage of cells positive to targeted protein. Using ×40 microscope objective, 8 randomly selected fields were analyzed for each section. Reproducibility of multiple sections from the same site was checked through the analysis of duplicates in a blind manner.

Enzyme linked immunosorbent assay. ELISA assays were performed to examine the protein expression of VEGF, IL-1ß, and TNF-α in the homogenates of pouch membrane using commercial kits (R&D) following manufacturer's instructions.

Gene expression of VEGF, IL-1ß, and TNF-α. Total RNA from pouch homogenates was reverse transcribed to cDNA as described[18]. Real-time quantitative reverse transcriptase-polymerase chain reaction (RT-PCR) was used to determine the gene levels by using ABI Prism® 7700 Sequence Detection System (PE-Applied Biosystems, Foster City, CA, USA). Primers for mouse IL-1ß and TNF-α were used as described[19]. Primers for mouse VEGF are: forward primer, 5'-TTA CTG CTG TAC CTC CAC C-3', and reverse primer, 5'-ACA GGA CGG CTT GAA GAT G-3'. Real-time RT-PCR was performed using Sybr® Green PCR Master reagents (PE-Applied Biosystems). Reactions were performed in a 25 μl volume with 0.5 μm primers. PCR cycles consisted of an initial denaturation step at 95ºC for 5 min, followed by 40 cycles of a 95ºC denaturation for 15 s, 60ºC annealing for 1 min. PCR amplification of the housekeeping gene, mouse GADPH, was run concurrently with the target gene (e.g., VEGF) each time as a control of sample loading and normalization between samples. The specificity of the

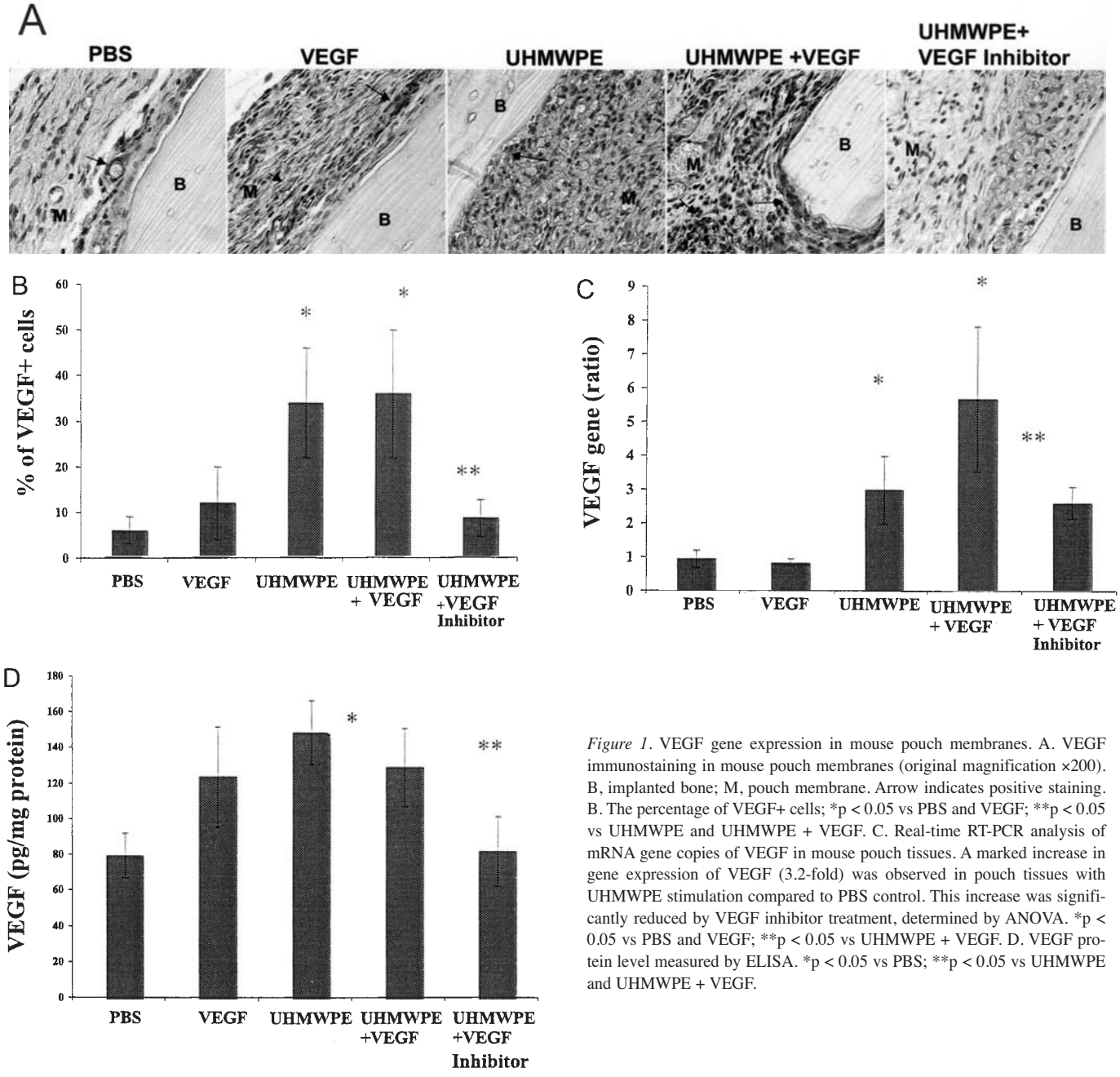

Figure 1. VEGF gene expression in mouse pouch membranes. A. VEGF immunostaining in mouse pouch membranes (original magnification ×200). B, implanted bone; M, pouch membrane. Arrow indicates positive staining. B. The percentage of VEGF+ cells; *$p < 0.05$ vs PBS and VEGF; **$p < 0.05$ vs UHMWPE and UHMWPE + VEGF. C. Real-time RT-PCR analysis of mRNA gene copies of VEGF in mouse pouch tissues. A marked increase in gene expression of VEGF (3.2-fold) was observed in pouch tissues with UHMWPE stimulation compared to PBS control. This increase was significantly reduced by VEGF inhibitor treatment, determined by ANOVA. *$p < 0.05$ vs PBS and VEGF; **$p < 0.05$ vs UHMWPE + VEGF. D. VEGF protein level measured by ELISA. *$p < 0.05$ vs PBS; **$p < 0.05$ vs UHMWPE and UHMWPE + VEGF.

amplification reactions was confirmed by agarose gel electrophoresis. To determine the relative level of gene expression for both target and the housekeeping genes, the comparative C_T (threshold cycle) method with arithmetic formulas was used. Subtracting the C_T of the housekeeping gene from the C_T of target gene yields the ΔC_T in each group (control and experimental groups), which was entered into the equation $2^{-\Delta CT}$ and calculated for the exponential amplification of PCR. Gene activity in the control group (PBS) was arbitrarily assigned the value of 1 to serve as reference. The expression of the target gene from experimental groups therefore represents the fold-difference expression relative to the reference gene.

Statistical analysis. Statistical analysis among groups was performed by the ANOVA test, with the Schafer formula for post hoc multiple comparisons, using the SPSS software package (version 7.5; SPSS Inc., Chicago, IL, USA). Data were expressed as mean ± standard error of the mean. A difference was considered significant at $p < 0.05$.

RESULTS

Effects of VEGF therapy. The mice used in this study tolerated both the surgery and drug treatment well. No mice were excluded from this study because of body weight loss, drug toxicity, or pouch infection.

Expression of VEGF in mouse pouch tissues. To determine the extent to which VEGF was induced by *in vivo* UHMWPE par-

ticle stimulation, we used semiquantitative immunostaining techniques to evaluate the tissue location of VEGF in pouch membranes. Figure 1A shows intense VEGF staining in UHMWPE-stimulated pouches, compared with saline control pouch membranes. VEGF staining was observed predominantly in the UHMWPE deposit foci surrounded by inflammatory cells. VEGF treatment exerted little effect on VEGF staining, either in the presence or absence of UHMWPE stimulation. However, VEGF staining was significantly diminished ($p < 0.05$) by VEGF inhibitor treatment (Figure 1B). Real-time RT-PCR assay (Figure 1C) revealed that significantly ($p < 0.05$) increased VEGF gene expression (3.2-fold) occurred in UHMWPE-stimulated pouches, as compared to saline controls. Although VEGF treatment slightly enhanced UHMWPE debris-induced VEGF gene expression, VEGF inhibitor treatment resulted in a remarkable ($p < 0.05$) reduction of VEGF gene expression, compared with untreated mice. VEGF protein expression in pouch membranes as evaluated by ELISA (Figure 1D) revealed that VEGF protein was increased in UHMWPE-stimulated pouches, compared with that seen in saline controls. VEGF inhibitor treatment suppressed VEGF protein production. Together, these data indicate that VEGF inhibition was effective in blocking UHMWPE-induced VEGF gene expression.

Effects of VEGF inhibitor on UHMWPE-induced tissue inflammation. Therapy using the VEGF inhibitor was observed to ameliorate UHMWPE particle-induced pouch tissue inflammation. As seen in Figure 2A, gross pathology verified that pouches injected with UHMWPE particles developed pronounced inflammatory changes, as compared with pouches injected with saline. Local injection of VEGF caused further deterioration of UHMWPE-stimulated tissue inflammation. VEGF inhibitor treatment significantly suppressed pouch tissue inflammation. Image analysis of sections (Figure 2B and 3) revealed that UHMWPE stimulation significantly increased both membrane thickness and the number of infiltrating cells in pouches, as compared to saline controls ($p < 0.05$). VEGF inhibitor treatment resulted in significant suppression of UHMWPE-induced cellular infiltration and membrane thickness (both $p < 0.05$). VEGF treatment slightly increased cellular infiltration, compared with untreated mice, although the increase did not reach statistical significance. UHMWPE particle-stimulated tissue inflammation was invariably accompanied by local accumulation of proinflammatory cytokines, such as IL-1ß and TNF-α[14]. As seen in Figure 4A, immunostaining analysis revealed that increased staining of both IL-1 and TNF occurred in pouches containing UHMWPE, compared with saline controls. Staining for these cytokines in UHMWPE stimulated pouches was predominantly located within the cytoplasm of inflammatory cell aggregates. Intense staining of IL-1 and TNF was significantly reduced by VEGF inhibitor treatment. Real-time RT-PCR assay (Figure 4B) showed that exposure to UHMWPE particles significantly increased gene expression of both IL-1ß (3-fold) and TNF-α (15-fold) in the pouch tissue, compared with controls (both $p < 0.05$). VEGF treatment had little effect on IL-1ß gene expression, but significantly increased TNF-α gene levels in pouches containing UHMWPE. In contrast, VEGF inhibitor treatment significantly reduced the gene levels of both IL-1ß and TNF-α in pouches containing UHMWPE ($p < 0.05$). When IL-1ß and TNF-α protein were also measured in the supernatants of pouch homogenates by ELISA assay (Figure 4C), similar protein expression profiles were found. These data verify that VEGF inhibitor treatment reduced UHMWPE particle-stimulated inflammatory

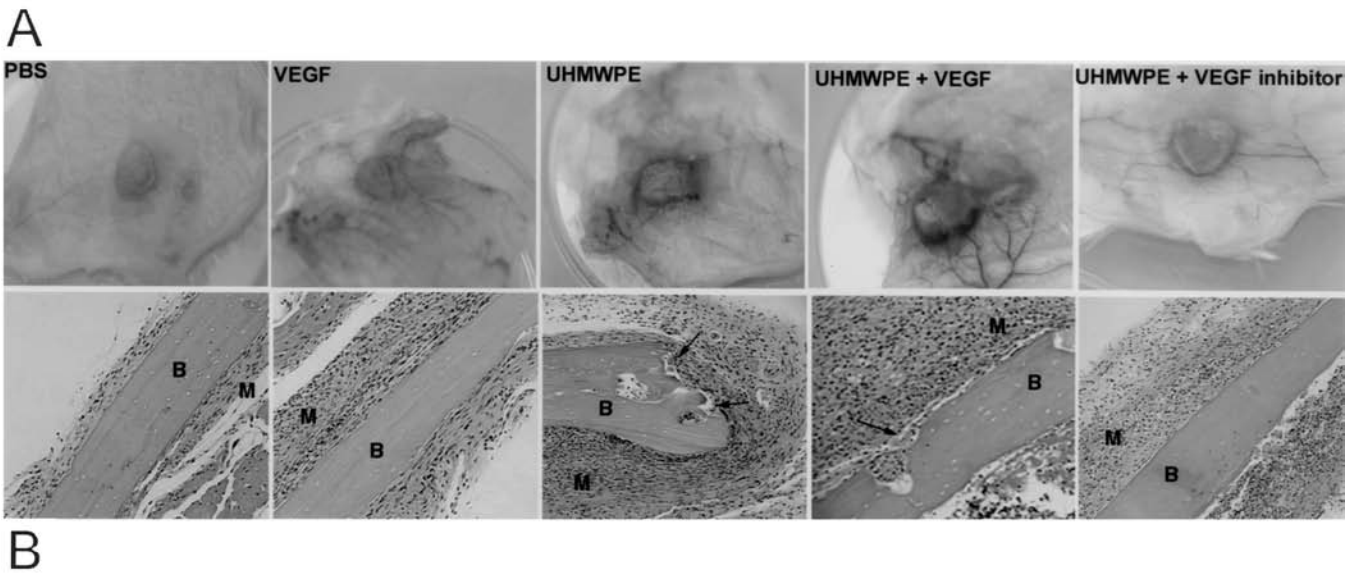

Figure 2. Representative pouch tissue histology of both macroscopic (A) and microscopic (B) appearance. All the main micrographs (B) are tissue sections stained with H&E (original magnification ×100). B, implanted bone; M, pouch membrane. Note the significant inflammatory cellular infiltration, proliferated pouch membrane, and foci erosions of implanted calvaria bone (arrows), while dramatic improvement of inflammatory osteolysis can be observed after VEGF inhibitor treatment.

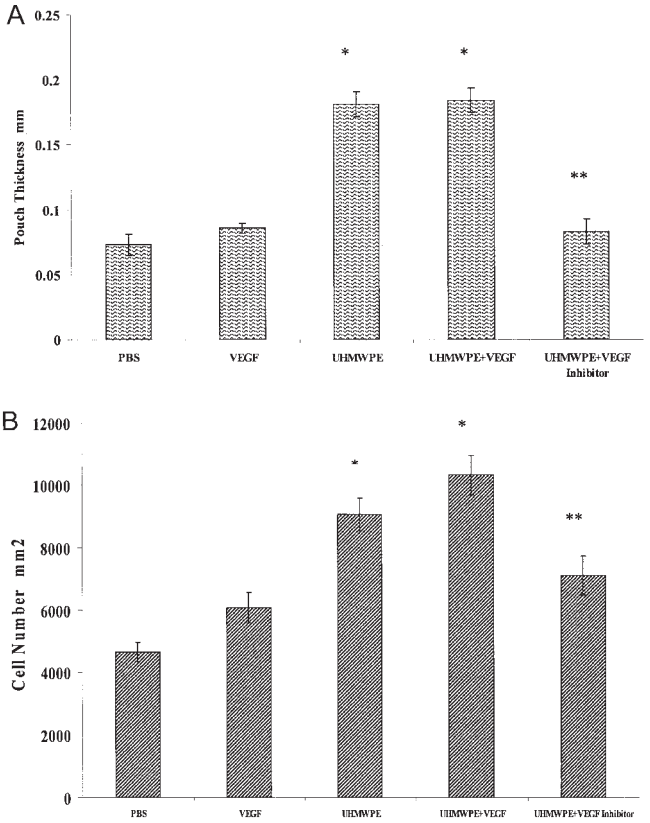

Figure 3. Histological assessment of UHMWPE–stimulated pouch membrane thickness (A) and total cell counts (B). Minimum of 3 separate sections per specimen were evaluated in a blinded fashion using Image-Pro software. A. *p < 0.05 vs PBS and VEGF; **p < 0.05 vs UHMWPE and UHMWPE + VEGF. B. *p < 0.05 vs PBS; **p < 0.05 vs UHMWPE and UHMWPE + VEGF.

cytokine production and significantly ameliorated tissue inflammation.

Effects of VEGF inhibitor on UHMWPE-induced osteoclastic bone resorption. Enhanced osteoclastogenesis has been recognized as a hallmark of various forms of osteoporosis, including the bone loss that occurs in AL[20]. We recently demonstrated an association of UHMWPE particle-induced tissue inflammation and enhanced osteoclastogenesis in this mouse model[19]. Histochemical TRAP staining was used to address whether UHMWPE particle-induced inflammatory osteoclastogenesis can be regulated by VEGF or VEGF inhibitor treatment. Figure 5 shows a discrete focus of TRAP staining observed on implanted calvaria bone surface in pouches with saline injection (control). The bone morphology remained essentially intact, and no resorption lacunae were observed. Pouches stimulated by UHMWPE resulted in intense TRAP staining on implanted bone surface, which extended into adjacent areas. Regions where TRAP+ cells localized were often pitted, suggesting active osteoclastic bone resorption. VEGF inhibitor treatment caused a significant reduction in the number of TRAP+ cells, and the bone resorption lacunae were significantly ameliorated. We also observed that VEGF treatment increased TRAP+ cells in pouches with or without UHMWPE particle stimulation, suggesting that VEGF orchestrates the development of osteoclastogenesis. As described[14], analysis of H&E-stained bone-implanted pouch sections revealed the frequent occurrence of implanted bone cortex erosions that occurred in close contact with particle-stimulated inflammatory pouch membranes (Figure 2B). Bone erosions were essentially undetectable in mice with VEGF inhibitor treatment, despite the exposure to the UHMWPE particles. Van Gieson stain was performed to quantify relative bone matrix collagen depletion using computerized image analysis, and Figure 6A shows representative images. UHMWPE particle stimulation dramatically increased the loss of bone collagen content at the bone surface in close contact with the inflammatory pouch membranes, in comparison with the bone collagen changes in sections from saline control pouches. VEGF inhibitor treatment resulted in the marked preservation of bone collagen content, exhibiting a pattern similar to results seen in saline controls. Computerized image analysis quantitatively determined the extent of collagen degradation (Figure 6B; $p < 0.05$). This suggests that VEGF inhibitor treatment effectively prevented bone collagen depletion stimulated by UHMWPE particles.

DISCUSSION

Our study revealed that exposure of UHMWPE particles increases VEGF expression (both mRNA and protein) in a mouse osteolysis model. Immunostaining revealed that intense VEGF staining predominantly around deposits of UHMWPE particles surrounded by inflammatory cells. VEGF inhibitor treatment suppressed inflammation of pouch tissue stimulated by UHMWPE particles, including activity of cellular infiltration, pouch membrane proliferation, and inflammatory cytokine production. Moreover, VEGF inhibitor treatment resulted in a significant reduction in the number of TRAP+ cells, and effectively prevented UHMWPE particle-stimulated collagen depletion and reduced the frequency of bone erosions in implanted bone.

The progression of AL is associated with the formation of a vascularized granulomatous tissue[4]. A pro-angiogenetic status in the loosening periprosthetic tissue augments the inflammatory response to wear debris[4,21]. The cellular mechanisms triggering this angiogenesis change are poorly characterized, but numerous pro-angiogenetic factors have been detected[21-23] in loosening periprosthetic tissues. VEGF is one of the most powerful angiogenetic agents known[5], and an association of VEGF expression in loose periprosthetic tissues has been recently observed. Jell and Al-Saffar[24] found that VEGF was expressed in all periprosthetic tissues, and intense VEGF staining was found on both macrophages and multinucleated giant cells within the implant lining layer, associated with the deposit of wear debris. Miyanishi, *et al*[21] reported that VEGF is overexpressed in loosening periprosthetic tissues. Double

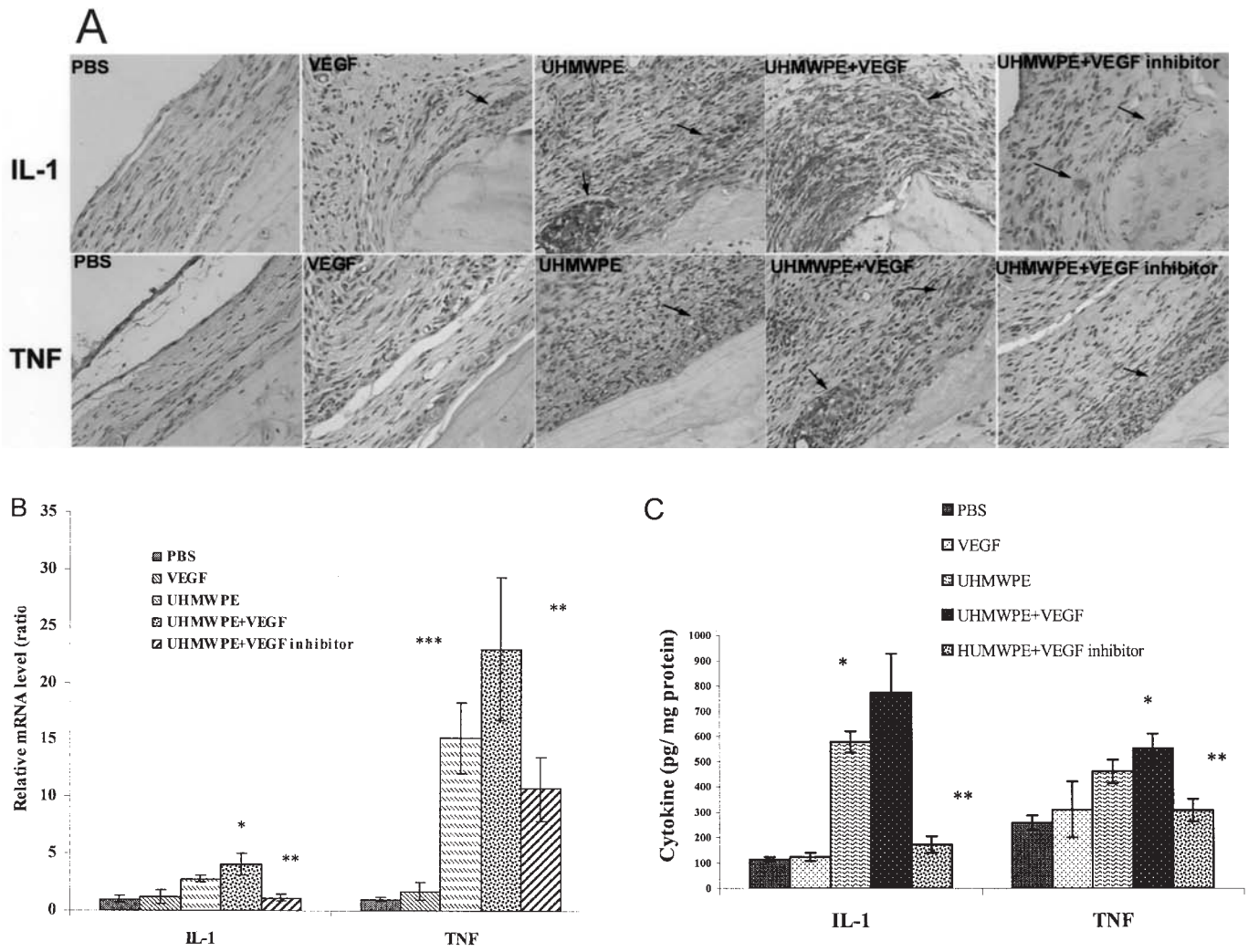

Figure 4. Gene expression of IL-1 and TNF in pouch membranes. A. Immunohistochemical staining of IL-1 and TNF in pouch membranes (original magnification ×200). B. RT-PCR analysis of mRNA copies of IL-1 and TNF. UHMWPE particles increased gene expression of IL-1 (3-fold) and TNF (15-fold) in pouch tissues compared to PBS control. This increase was significantly reduced by VEGF inhibitor treatment. *$p < 0.05$ vs PBS; **$p < 0.05$ vs UHMWPE and UHMWPE + VEGF; ***$p < 0.05$ vs PBS, VEGF, and UHMWPE + VEGF. C. The protein level of IL-1 and TNF in the supernatants of the pouch membrane homogenates was measured by ELISA. *$p < 0.05$ vs PBS; **$p < 0.05$ vs UHMWPE and UHMWPE + VEGF.

immunofluorescent staining demonstrated that VEGF staining was colocalized with CD11b-positive macrophages. Further, they found that supernatants from titanium particle-challenged monocyte/macrophages significantly increased macrophage chemotactic activity, which could be inhibited by anti-VEGF neutralizing antibody. Our study shows that VEGF expression (mRNA and protein) is significantly increased after UHMWPE particle stimulation. This may support the concept that VEGF plays a significant role in the early events of AL development, including implant wear-induced inflammatory osteolysis, as evidenced in our study. The reason why VEGF inhibitor significantly reduced VEGF gene expression might be due to the amelioration of the tissue inflammation. Our data show that VEGF inhibitor significantly diminished UHMWPE-induced tissue inflammation, including the reduction of inflammatory cells, predominantly macrophages, the main VEGF-producing cells[5,6]. Using double immunofluorescent staining, we showed that CD68 (a macrophage marker) was colocalized with VEGF staining, indicating that activated macrophages comprise the major source of VEGF expression in inflammatory pouch tissue (data not shown).

Multiple lines of evidence indicate that VEGF is critically involved in the initiation and persistence of inflammation[11,25–30]: (1) Clinical studies have demonstrated a close association of tissue VEGF expression with tissue inflammation status in osteoarthritis[28] and rheumatoid arthritis[25,27], with similar findings in prosthetic loosening[21,24]. (2) Using mouse collagen type II-induced arthritis as a model, Luttun, *et al*[30] reported that treatment with anti-VEGF receptor I antibody significantly reduced the incidence and severity of joint disease. De Bandt, *et al*[26] obtained similar results in a transgenic K/B×N mouse model of rheumatoid arthritis. Our data

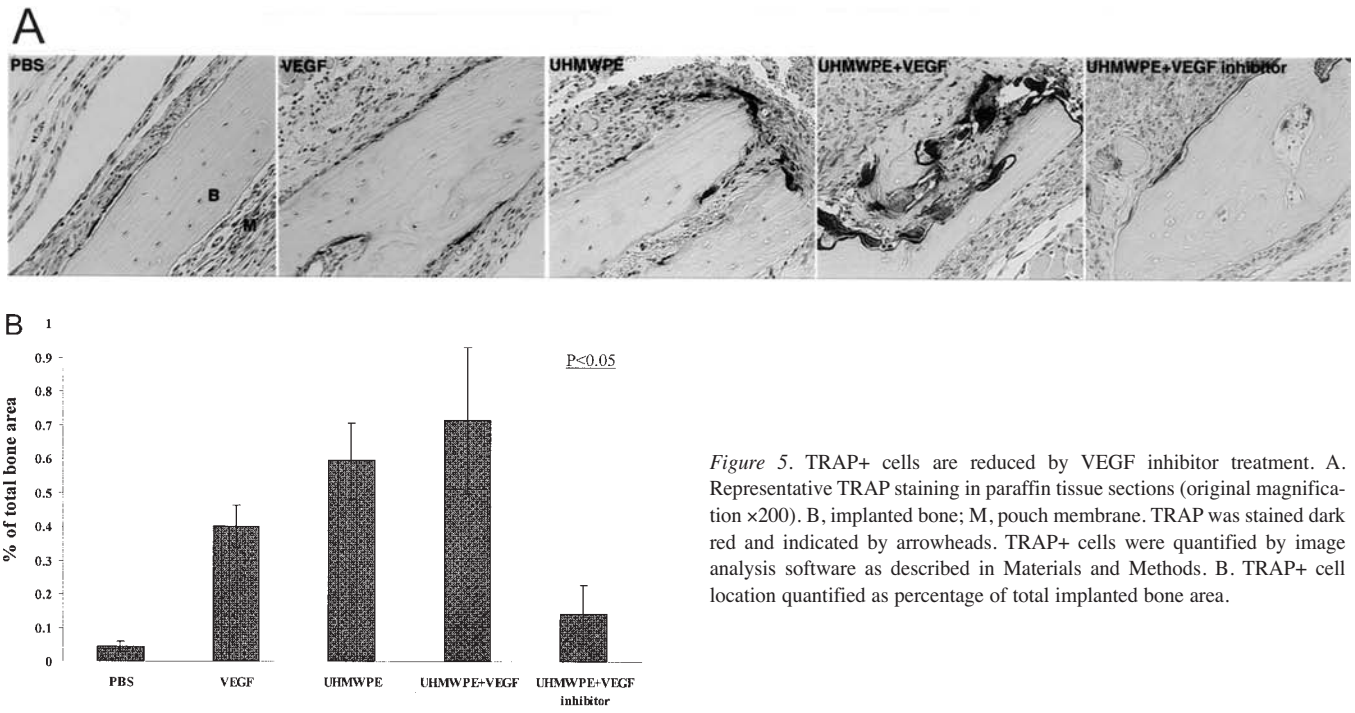

Figure 5. TRAP+ cells are reduced by VEGF inhibitor treatment. A. Representative TRAP staining in paraffin tissue sections (original magnification ×200). B, implanted bone; M, pouch membrane. TRAP was stained dark red and indicated by arrowheads. TRAP+ cells were quantified by image analysis software as described in Materials and Methods. B. TRAP+ cell location quantified as percentage of total implanted bone area.

demonstrated that neutralization of VEGF activity significantly diminished tissue inflammation, which is in good agreement with these findings. VEGF gene expression is upregulated by inflammatory cytokines, such as IL-1[31,32] and TNF[33,34]. Since IL-1 and TNF are among the major cytokines detected in periprosthetic tissue[23,35] and are known to be potent mediators of the bone resorption associated with AL[36], the regulatory mechanisms of VEGF by these cytokines in the setting of progression of AL represents an area of significant interest. This study shows that VEGF inhibitor treatment suppresses tissue inflammation stimulated by UHMWPE particles and reduces the level of IL-1ß and TNF-α in UHMWPE-

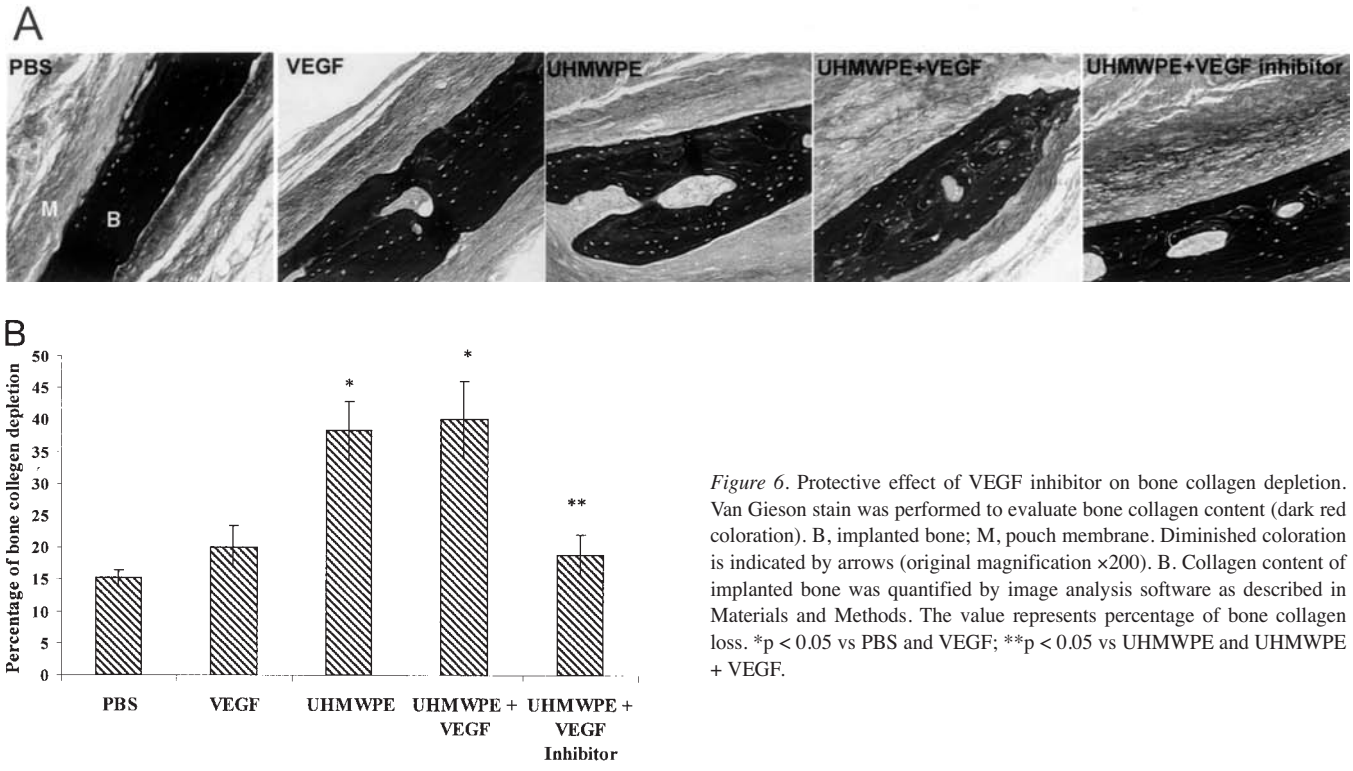

Figure 6. Protective effect of VEGF inhibitor on bone collagen depletion. Van Gieson stain was performed to evaluate bone collagen content (dark red coloration). B, implanted bone; M, pouch membrane. Diminished coloration is indicated by arrows (original magnification ×200). B. Collagen content of implanted bone was quantified by image analysis software as described in Materials and Methods. The value represents percentage of bone collagen loss. *p < 0.05 vs PBS and VEGF; **p < 0.05 vs UHMWPE and UHMWPE + VEGF.

stimulated pouch tissues. The molecular mechanism of the effect of VEGF inhibitor is still unclear. VEGF appears to exert inflammatory effects through binding to its receptors, especially Flt-1. In addition to endothelial cells, Flt-1 is expressed on cells of the monocyte-macrophage lineage and is involved in macrophage activation (IL-1ß and TNF-α expression)[37], migration[38,39], and differentiation[12,40]. We hypothesize that the effectiveness of VEGF inhibitor treatment is due to downregulation of VEGF/Flt-1 signaling activation induced by wear debris. Our previous experiments (unpublished data) have shown that UHMWPE particles first increased Flt-1 gene expression in cultured mouse macrophages, which was then inhibited by VEGF inhibitor treatment. In addition, we also find that a positive association does exist between the Flt-1 gene level and pouch tissue inflammation status (unpublished data). The inhibition of inflammation mediated by VEGF within the pouch tissue is an attractive approach in treatment of AL, because it can prevent the formation of chronic inflammation provoked by wear debris in the periprosthetic tissue, especially at the early stage of development of AL.

We have also demonstrated that VEGF inhibitor treatment abrogated UHMWPE particle-stimulated osteoclastogenesis and bone degradation. The biological role of VEGF in the development of osteolysis may be related to its overlapping interactions with endothelial cells, monocytes, and osteoclasts. VEGF increases both endothelial cell proliferation and vascular permeability, which may contribute to the development of high vascularization in loosening periprosthetic tissues[4,21]. A chemotactic study[21] revealed that supernatants from titanium particle-challenged inflammatory cells significantly increased macrophage migration, and anti-human VEGF neutralizing antibody significantly suppressed this chemotactic activity. This observation indicated that the local accumulation of VEGF in the loosening periprosthetic tissue may contribute to the recruitment of macrophages to the bone-implant interface in an autocrine/paracrine manner. Recent reports of a linkage between VEGF activity and osteoclastogenesis indicate that stimulated endothelial cells produce receptor activator of nuclear factor-κB (RANK), a protein critical in initiating osteoclastogenesis[41] and the biological activity of macrophage colony-stimulating factor[40,42] in osteoclastogenesis. VEGF may also stimulate osteoclast recruitment[40], differentiation[43], activation, and survival[12]. We hypothesize that the effectiveness of VEGF inhibitor treatment in reduction of TRAP+ cells is due to the reduction of infiltrating macrophages (the osteoclast precursor cells) and the reduction of local RANKL production. We have found that VEGF inhibitor treatment significantly decreased UHMWPE particle-induced RANK and RANKL gene expression using the same mouse model (data not shown), suggesting that VEGF has a role in regulation of RANK/RANKL-mediated osteoclastogenesis.

We should point out that one limitation of this mouse model is the lack of blood supplies to implanted bone. Implanted bone will deteriorate after extended periods of implantation without vascular supply. We observed that beyond 14 days of implantation, the overall degradation of implanted bone collagen masked UHMWPE particle-associated bone resorption[14]. This observation restricts the model to the study of acute osteolysis, rather than the chronic osteolysis seen in aseptic loosening.

Despite this limitation, our model appears to be useful for basic *in vivo* investigations of cellular response to wear debris under controlled experimental conditions, and for screening therapeutic agents/therapy for debris-associated bone resorption. As well, the potential complications of VEGF inhibitor treatment need to be evaluated further.

In summary, the observation that VEGF inhibitor treatment prevented UHMWPE particle-induced inflammatory osteolysis opens new possibilities for treatment of AL, especially in the early stages. Since other inflammatory cytokines such as IL-1ß and TNF-α are known to be potent mediators of bone resorption associated with AL[36], it might be most effective if an anti-VEGF therapy was combined with an antiinflammatory therapeutic strategy such as TNF-α inhibition.

REFERENCES

1. Berry DJ, Harmsen WS, Cabanela ME, Morrey BF. Twenty-five-year survivorship of two thousand consecutive primary Charnley total hip replacements: Factors affecting survivorship of acetabular and femoral components. J Bone Joint Surg Am 2002;84:171-7.
2. Keener JD, Callaghan JJ, Goetz DD, et al. Twenty-five-year results after Charnley total hip arthroplasty in patients less than fifty years old: a concise follow-up of a previous report. J Bone Joint Surg Am 2003;85:1066-72.
3. Bauer TW. Particles and peri-implant bone resorption. Clin Orthop 2002;405:138-43.
4. Al Saffar N, Mah JT, Kadoya Y, Revell PA. Neovascularisation and the induction of cell adhesion molecules in response to degradation products from orthopaedic implants. Ann Rheum Dis 1995; 54:201-8.
5. Goodsell DS. The molecular perspective: VEGF and angiogenesis. Oncologist 2002;7:569-70.
6. Harry LE, Paleolog EM. From the cradle to the clinic: VEGF in developmental, physiological, and pathological angiogenesis. Birth Defects Res Part C Embryo Today 2003;69:363-74.
7. Ferrara N, Davis-Smyth T. The biology of vascular endothelial growth factor. Endocr Rev 1997;18:4-25.
8. Tombran-Tink J, Barnstable CJ. Osteoblasts and osteoclasts express PEDF, VEGF-A isoforms, and VEGF receptors: possible mediators of angiogenesis and matrix remodeling in the bone. Biochem Biophys Res Commun 2004;316:573-9.
9. Vinores SA, Xiao WH, Zimmerman R, et al. Upregulation of vascular endothelial growth factor (VEGF) in the retinas of transgenic mice overexpressing interleukin-1 beta (IL-1 beta) in the lens and mice undergoing retinal degeneration. Histol Histopathol 2003;18:797-810.
10. Waltenberger J, Claesson-Welsh L, Siegbahn A, et al. Different signal transduction properties of KDR and Flt1, two receptors for vascular endothelial growth factor. J Biol Chem 1994;269:26988-95.
11. Kunstfeld R, Hirakawa S, Hong YK, et al. Induction of cutaneous delayed-type hypersensitivity reactions in VEGF-A transgenic mice results in chronic skin inflammation associated with persistent

lymphatic hyperplasia. Blood 2004;104:1048-57.
12. Nakagawa M, Kaneda T, Arakawa T, et al. Vascular endothelial growth factor (VEGF) directly enhances osteoclastic bone resorption and survival of mature osteoclasts. FEBS Lett 2000;473:161-4.
13. Henriksen K, Karsdal M, Delaisse JM, Engsig MT. RANKL and vascular endothelial growth factor (VEGF) induce osteoclast chemotaxis through an ERK1/2-dependent mechanism. J Biol Chem 2003;278:48745-53.
14. Ren WP, Yang S, Wooley PH. A novel murine model of orthopaedic wear debris-associated osteolysis. Scand J Rheumatology 2004;33:1-10.
15. Wooley PH, Morren R, Andary J, et al. Inflammatory responses to orthopaedic biomaterials in the murine air pouch. Biomaterials 2002;23:517-26.
16. Liao F, Schenkel AR, Muller WA. Transgenic mice expressing different levels of soluble platelet/endothelial cell adhesion molecule-IgG display distinct inflammatory phenotypes. J Immunol 1999;163:5640-8.
17. Ren WP, Wu B, Mayton L, Wooley PH. Polyethylene and methyl methacrylate particle-stimulated inflammatory tissue and macrophages up-regulate bone resorption in a murine neonatal calvaria in vitro organ system. J Orthop Res 2002;20:1031-7.
18. Yang SY, Ren W, Park Y, et al. Diverse cellular and apoptotic responses to variant shapes of UHMWPE particles in a murine model of inflammation. Biomaterials 2002;23:3535-43.
19. Ren WP, Yang SY, Fang HW, et al. Distinct gene expression of receptor activator of nuclear factor-kB and rank ligand in the inflammatory response to variant morphologies of UHMWPE particles. Biomaterials 2003;24:4819-26.
20. Wooley PH, Schwarz EM. Aseptic loosening. Gene Ther 2004;11:402-7.
21. Miyanishi K, Trindade MC, Ma T, et al. Periprosthetic osteolysis: induction of vascular endothelial growth factor from human monocyte/macrophages by orthopaedic biomaterial particles. J Bone Miner Res 2003;18:1573-83.
22. Gallo J, Kaminek P, Ticha V, et al. Particle disease. A comprehensive theory of periprosthetic osteolysis: a review. Biomed Pap Med Fac Univ Palacky Olomouc Czech Repub 2002;146:21-8.
23. Jones LC, Frondoza C, Hungerford DS. Immunohistochemical evaluation of interface membranes from failed cemented and uncemented acetabular components. J Biomed Mater Res 1999;48:889-98.
24. Jell GM, Al-Saffar N. Does a pro-angiogenic state exist in the bone-implant interface of aseptically loosened joint prosthesis? J Mater Sci Mater Med 2001;12:1069-73.
25. Ikeda M, Hosoda Y, Hirose S, et al. Expression of vascular endothelial growth factor isoforms and their receptors Flt-1, KDR, and neuropilin-1 in synovial tissues of rheumatoid arthritis. J Pathol 2000;191:426-33.
26. De Bandt M, Ben Mahdi MH, Ollivier V, et al. Blockade of vascular endothelial growth factor receptor I (VEGF-RI), but not VEGF-RII, suppresses joint destruction in the K/BxN model of rheumatoid arthritis. J Immunol 2003;171:4853-9.
27. Fava RA, Olsen NJ, Spencer-Green G, et al. Vascular permeability factor/endothelial growth factor (VPF/VEGF): accumulation and expression in human synovial fluids and rheumatoid synovial tissue. J Exp Med 1994;180:341-6.
28. Haywood L, McWilliams DF, Pearson CI, et al. Inflammation and angiogenesis in osteoarthritis. Arthritis Rheum 2003;48:2173-7.
29. Xia YP, Li B, Hylton D, et al. Transgenic delivery of VEGF to mouse skin leads to an inflammatory condition resembling human psoriasis. Blood 2003;102:161-8.
30. Luttun A, Tjwa M, Carmeliet P. Placental growth factor (PlGF) and its receptor Flt-1 (VEGFR-1): novel therapeutic targets for angiogenic disorders. Ann NY Acad Sci 2002;979:80-93.
31. Ben Av P, Crofford LJ, Wilder RL, Hla T. Induction of vascular endothelial growth factor expression in synovial fibroblasts by prostaglandin E and interleukin-1: a potential mechanism for inflammatory angiogenesis. FEBS Lett 1995;372:83-7.
32. Salven P, Hattori K, Heissig B, Rafii S. Interleukin-1 alpha promotes angiogenesis in vivo via VEGFR-2 pathway by inducing inflammatory cell VEGF synthesis and secretion. FASEB J 2002;16:1471-3.
33. Paleolog EM, Young S, Stark AC, et al. Modulation of angiogenic vascular endothelial growth factor by tumor necrosis factor alpha and interleukin-1 in rheumatoid arthritis. Arthritis Rheum 1998;41:1258-65.
34. Kato T, Haro H, Komori H, Shinomiya K. Sequential dynamics of inflammatory cytokine, angiogenesis inducing factor and matrix degrading enzymes during spontaneous resorption of the herniated disc. J Orthop Res 2004;22:895-900.
35. Stea S, Visentin M, Granchi D, et al. Cytokines and osteolysis around total hip prostheses. Cytokine 2000;12:1575-9.
36. Childs LM, Goater JJ, O'Keefe RJ, Schwarz EM. Efficacy of etanercept for wear debris-induced osteolysis. J Bone Miner Res 2001;16:338-47.
37. Sawano A, Iwai S, Sakurai Y, et al. Flt-1, vascular endothelial growth factor receptor 1, is a novel cell surface marker for the lineage of monocyte-macrophages in humans. Blood 2001; 97:785-91.
38. Barleon B, Sozzani S, Zhou D, et al. Migration of human monocytes in response to vascular endothelial growth factor (VEGF) is mediated via the VEGF receptor flt-1. Blood 1996;87:3336-43.
39. Matsumoto Y, Tanaka K, Hirata G, et al. Possible involvement of the vascular endothelial growth factor-Flt-1-focal adhesion kinase pathway in chemotaxis and the cell proliferation of osteoclast precursor cells in arthritic joints. J Immunol 2002;168:5824-31.
40. Niida S, Kaku M, Amano H, et al. Vascular endothelial growth factor can substitute for macrophage colony-stimulating factor in the support of osteoclastic bone resorption. J Exp Med 1999;190:293-8.
41. Min JK, Kim YM, Kim YM, et al. Vascular endothelial growth factor up-regulates expression of receptor activator of NF-kappa B (RANK) in endothelial cells. Concomitant increase of angiogenic responses to RANK ligand. J Biol Chem 2003;278:39548-57.
42. Kodama I, Niida S, Sanada M, et al. Estrogen regulates the production of VEGF for osteoclast formation and activity in op/op mice. J Bone Miner Res 2004;19:200-6.
43. Kaku M, Kohno S, Kawata T, et al. Effects of vascular endothelial growth factor on osteoclast induction during tooth movement in mice. J Dent Res 2001;80:1880-3.